

Geophysical Research Letters[®]



RESEARCH LETTER

10.1029/2021GL094761

Key Points:

- Stronger and more realistic Southern Ocean phytoplankton activity by modeling iron release from melting continental and sea ice
- Continental and sea ice iron sources have an overall additive effect on the biological carbon pump strength
- The fertilization effects of the sea-ice iron source are larger when the continental-ice iron source is activated

Supporting Information:

Supporting Information may be found in the online version of this article.

Correspondence to:

R. Person,
renaud.person@ird.fr

Citation:

Person, R., Vancoppenolle, M., Aumont, O., & Malsang, M. (2021). Continental and sea ice iron sources fertilize the Southern Ocean in synergy. *Geophysical Research Letters*, 48, e2021GL094761. <https://doi.org/10.1029/2021GL094761>

Received 9 JUN 2021
Accepted 12 NOV 2021

Author Contributions:

Conceptualization: Renaud Person, Martin Vancoppenolle, Olivier Aumont
Data curation: Renaud Person
Formal analysis: Renaud Person, Manon Malsang
Funding acquisition: Martin Vancoppenolle, Olivier Aumont
Investigation: Renaud Person, Manon Malsang
Methodology: Renaud Person, Martin Vancoppenolle, Olivier Aumont
Resources: Renaud Person, Martin Vancoppenolle, Olivier Aumont
Software: Renaud Person, Martin Vancoppenolle, Olivier Aumont
Supervision: Renaud Person, Martin Vancoppenolle, Olivier Aumont

© 2021 The Authors.

This is an open access article under the terms of the [Creative Commons Attribution-NonCommercial License](https://creativecommons.org/licenses/by/4.0/), which permits use, distribution and reproduction in any medium, provided the original work is properly cited and is not used for commercial purposes.

Continental and Sea Ice Iron Sources Fertilize the Southern Ocean in Synergy

Renaud Person^{1,2} , Martin Vancoppenolle² , Olivier Aumont² , and Manon Malsang³

¹Sorbonne Université, CNRS, IRD, MNHN, INRAE, ENS, OSU Ecce Terra, Paris, France, ²Sorbonne Université, CNRS, IRD, MNHN, LOCEAN-IPSL, Paris, France, ³Département de Géosciences, Ecole Normale Supérieure, Université PSL, Paris, France

Abstract Iron release from melting continental and sea ice is deemed important for phytoplankton, the growth of which is iron-limited in the Southern Ocean. Both sources are generally considered separately, yet their effects on the biological carbon pump could interact. Using a global ocean-sea-ice-biogeochemical model with a representation of both continental and sea ice iron sources, we find them to have an overall additive effect on phytoplankton activity, increasing carbon export by +13.9% of the Southern Ocean total, with continental ice contributing +4.5% and sea ice +8.0%. The +1.4% residual is due to a coupled fertilization effect: When the iron source from continental ice is activated, iron in sea ice increases by 16%, so does iron transport toward low production areas. Overall, this increases phytoplankton activity: Fertilization is more efficient where sea ice melts than at locations of initial iron release by continental ice.

Plain Language Summary Phytoplankton refers to micro-algae growing and drifting within seawater. Most living organisms in the ocean ultimately depend on phytoplankton. When sinking, organic matter produced by phytoplankton sequesters large amounts of carbon in the deep ocean. The Southern Ocean is a key area for these processes. There, the iron dissolved in seawater, available in tiny amounts, exerts a strong constraint on phytoplankton growth. Melting ice in the Southern Ocean is a key iron source to surface waters, which fosters phytoplankton growth, yet how much and how efficiently is the subject of ongoing research. Here we present numerical simulations of ocean physics, ice, and marine plankton, representing iron release from melting ice. We find more plankton and stronger carbon sequestration in the ocean where ice releases more iron. These locations also correspond to where phytoplankton are seen from space. A unique aspect of our simulations is the accounting for ice of two different origins (continental and sea ice). We find that both ice forms tend to release iron at similar locations. We also find their fertilization effects to reinforce each other. Indeed, sea ice stores iron released by continental ice and moves it where it is more efficiently assimilated by phytoplankton.

1. Introduction

The scarcity of iron (Fe) strongly limits photosynthesis in the Southern Ocean (SO) (Boyd et al., 2007; Martin, 1990). In this High Nutrient Low Chlorophyll ocean, sea ice, icebergs and ice shelves are considered important sources of Fe (Boyd & Ellwood, 2010). However, their respective roles differ: melting icebergs and ice shelves act as annually continuous external sources of Fe (Hopwood et al., 2019; St-Laurent et al., 2017) while sea ice extracts Fe from seawater in fall and winter from coastal freezing sites and conveys it to melting sites, where release is maximum in spring or summer (Lancelot et al., 2009; Lannuzel et al., 2016), stimulating ice-edge phytoplankton development (Arrigo et al., 1997; Sedwick & DiTullio, 1997). The large sea-ice Fe inventory is generally attributed to suspended sediments (de Jong et al., 2013; Noble et al., 2013), as supported by model studies (Lancelot et al., 2009; Person et al., 2020). Physical (e.g., internal freezing) and biogeochemical processes in sea ice also affect Fe in sea ice (Lannuzel et al., 2016; Raiswell et al., 2018). Similarly, icebergs and ice shelves carry Fe from the Antarctic continent and release it into the ocean upon melting (Lin et al., 2011; St-Laurent et al., 2017). This Fe could also be stored into and transported by sea ice, a mechanism we investigate here.

Biogeochemical interactions between continental ice (ice shelves and icebergs) and sea ice have been suggested, mostly at regional scales. For instance, ice shelf basal melt rate largely explains primary production variance in the Antarctic polynyas (Arrigo et al., 2015; Dinniman et al., 2020), recognized regions of intense sea-ice production and export (e.g., Tamura et al., 2016). In addition, in situ observations near the Moscow University and

Validation: Renaud Person, Martin Vancoppenolle, Olivier Aumont

Visualization: Renaud Person, Manon Malsang

Writing – original draft: Renaud Person

Writing – review & editing: Renaud Person, Martin Vancoppenolle, Olivier Aumont, Manon Malsang

Totten Ice Shelves suggest the incorporation of Fe of glacial origin into growing sea ice (Duprat et al., 2020). On this basis, one could think that interactions between continental and sea ice Fe sources to the ocean could operate at the scale of the SO. Purely physical interactions between melting Antarctic icebergs or ice shelves and sea ice have been documented (Bintanja et al., 2013; Merino et al., 2016). However, model studies rarely considered continental and sea ice Fe sources together, if at all (Death et al., 2014; Lancelot et al., 2009; Laufkötter et al., 2018; Person et al., 2019, 2020; Wadley et al., 2014; Wang et al., 2014) and therefore may have missed possible synergies between them.

In this study, we question and explore the synergistic effects of Fe release from the different ice forms encountered in the SO (ice shelves, icebergs, and sea ice) on the biological carbon pump. We present simulations performed with an ocean-sea-ice-biogeochemistry model with active Fe sources from sea ice, icebergs, and ice shelves through recently developed representations (Person et al., 2019, 2020), which are based on recent observational compilations (Lannuzel et al., 2016; Raiswell et al., 2016). We find that the fertilization effects of continental and sea ice Fe sources are generally additive, and evidence for a coupling effect between them.

2. Method

2.1. Model Components

We use the ocean-sea-ice-biogeochemical model NEMO (Madec, 2008), version 3.6, in a global configuration with a nominal resolution of 1° and 75 vertical z-coordinate levels (Person et al., 2019). Ocean general circulation is represented using OPA, a hydrostatic, primitive equation ocean dynamical core (Madec, 2008). Sea ice is represented with the LIM 3.6 model (Rousset et al., 2015) which includes growth and melt, drift, transport, and deformation processes, in a multi-category tiling framework (Vancoppenolle et al., 2009). Sea ice and the surface ocean exchange heat, freshwater, and salt.

We use the PISCES model to represent the lower trophic levels of marine ecosystems and the biogeochemical cycles of carbon and of the main nutrients, in particular Fe (Aumont et al., 2015). PISCES explicitly represents two phytoplankton functional types, two zooplankton size classes, and 24 tracers overall. External sources of Fe from atmospheric dust, sediment, and rivers are included.

Icebergs and ice shelves are considered as external, prescribed, climatological, freshwater sources. The model-based freshwater flux from icebergs (Merino et al., 2016) based on recent observations (Depoorter et al., 2013) is released at the ocean surface. The ice shelf freshwater flux at the ice front is parameterized following Mathiot et al. (2017), emulating the effects of the unresolved sub-ice-shelf overturning circulation. The ice shelf freshwater flux is distributed from the ice front base down to the seabed or the grounding line. Continental and sea ice interact only indirectly, through changes in upper ocean salinity and temperature induced by freshwater from ice shelves and icebergs.

2.2. Continental and Sea Ice Iron Sources

Both continental and sea ice Fe sources implemented in our model were evaluated in Person et al. (2019, 2020). The Fe source of icebergs and ice shelves is represented by associating a sediment content of 0.5 g L⁻¹ to their freshwater fluxes. The soluble fraction of sedimentary Fe (ferrihydrite), of which 0.1% is estimated bioavailable, is set at 5% in the mid-range of uncertainties. A total annual Fe flux of 1.25 Gmol yr⁻¹ is simulated with similar contributions from icebergs and ice shelves. The iceberg Fe flux is homogeneously distributed over the first 120 m of the ocean. The ice shelf Fe flux is distributed as the ice shelf freshwater flux. Because ice shelf Fe is distributed along the ice front, sedimentary Fe resuspended by the overturning circulation in sub-ice-shelf cavities is not included. Our approach also implies that Fe from sub-ice-shelf cavities does not alter Fe concentrations outside the cavities, although this may be the case (Dinniman et al., 2020).

Iron in sea ice is modeled as a conservative, physically active, biologically and chemically passive, category-dependent, and vertically-constant sea-ice tracer (Person et al., 2020). Sea-ice Fe follows a conservation equation with all represented sea-ice physical processes (growth and melt, transport, and deformation). Iron is incorporated into sea ice upon growth in proportion to the Fe concentration in seawater. The associated exchange velocity (4×10^{-6} m s⁻¹) was adjusted to approach the best observational estimate of the mean sea-ice Fe content (Lannuzel et al., 2016). Iron release upon melting is assumed proportional to melt rate. Many possibly relevant

processes are ignored here (e.g., wind-driven dust deposition on sea ice, brine inclusions, physical, biological, and chemical processes within sea ice).

Continental and sea ice Fe sources are indirectly coupled because Fe fluxes from continental ice affect the surface ocean Fe concentration, on which the Fe incorporation flux into sea ice depends.

2.3. Experiments

Four experiments were designed to provide a comprehensive view of the fertilization effects by the whole Antarctic cryosphere on marine biogeochemistry. In the CTL experiment, considered as reference, there is no exchange of Fe between seawater and sea ice and no external source of Fe from icebergs and ice shelves. In the SI experiment, only sea ice-related Fe exchanges are active (Person et al., 2020). The AIS experiment only considers the Fe source of icebergs and ice shelves (Person et al., 2019). In the SI&AIS experiment, continental and sea ice Fe sources are active and thus their respective effects are coupled.

The experiments are initialized from the annual-mean climatologies of the World Ocean Atlas 2013 for temperature (Locarnini et al., 2013) and salinity (Zweng et al., 2013), World Ocean Atlas 2009 for nitrate, phosphate, silicate, and oxygen (Garcia et al., 2010a, 2010b) and GLODAP-v1 for DIC and alkalinity (Key et al., 2004). Iron is initialized from a previous simulation run to a quasi-steady state (Aumont et al., 2015). Sea-ice thickness, concentration, salinity, and temperature are set to constant values when sea surface temperature is lower than 2°C. Sea-ice Fe is initialized to 10 nmol L⁻¹ uniformly (Lannuzel et al., 2016). These experiments were run using the CORE-I normal year atmospheric forcing fields (Griffies et al., 2009) over a 50-year period to achieve a sufficient equilibrium state for the seasonal variations of the biogeochemical variables in the upper levels. Only the last year of simulation is analyzed.

3. Results

3.1. Iron From Melting Ice Increases Phytoplankton Activity

The spatial distribution of surface chlorophyll concentrations (SChl) from model experiments and observations is given in Figure 1, key summary statistics in Table 1. The SI&AIS experiment reproduces the typical finding that melting ice generally stimulates phytoplankton activity by releasing Fe (Lancelot et al., 2009; Laufkötter et al., 2018; Person et al., 2019, 2020), increasing SChl (Figure 1d) and annual PP and carbon export (by 7.3% and 13.9%, respectively).

Iron released by melting ice expands photosynthesis to zones devoid of any biological activity in the control run (Figure 1a), and detected as biologically active in satellite ocean color retrievals, for example, off Prydz Bay or in the Western Ross Sea (Figure 1e). This induces a remarkable shrinking of low production areas (Table 1), by 3–4 million km² or 25%–50% of their total area. This shrinking is sensitive to the annual primary production threshold used for the definition of the low production area (40 or 25 mg m⁻² yr⁻¹, Table 1). Overall, the effect of sea ice is 2–4 times larger than that of continental ice, despite an overall lower Fe release (Table 1).

The spatial patterns of SChl differences are driven by the response of phytoplankton to Fe release from melting ice. An important role is played by light and nutrient limitations, largely conditioned by sea-ice presence and mixed-layer depth. Fertilization by melting continental ice (AIS experiment, Figure 1c) is particularly efficient in a narrow band along the Antarctic coast and in the lee of the Antarctic Peninsula where iceberg melting is strongest. The sea-ice fertilization footprint (SI experiment, Figure 1b) is more spread out in comparison, spanning a rather wide band along Antarctica, with larger values east off the tip of the Antarctic Peninsula, off Prydz Bay and in the Western Ross Sea. There is no effect where sea ice persists in summer such as along the Ross or Weddell Sea coasts, or in remote ice-covered areas where the Fe content of sea ice is small (e.g., east of the Weddell Sea), or where mixing is too high (Figure 1b).

3.2. Continental and Sea Ice Iron Sources Differ but Share Similarities

Changes in SChl in our experiments ultimately stem from Fe fluxes from melting ice. Figure 2 gives the spatial distribution of annual Fe release for each separate ice source (Figures 2a and 2b) and for both sources combined (Figure 2c). Iron release largely reflects annual melting, itself largely related to the drift of the ice form of interest.

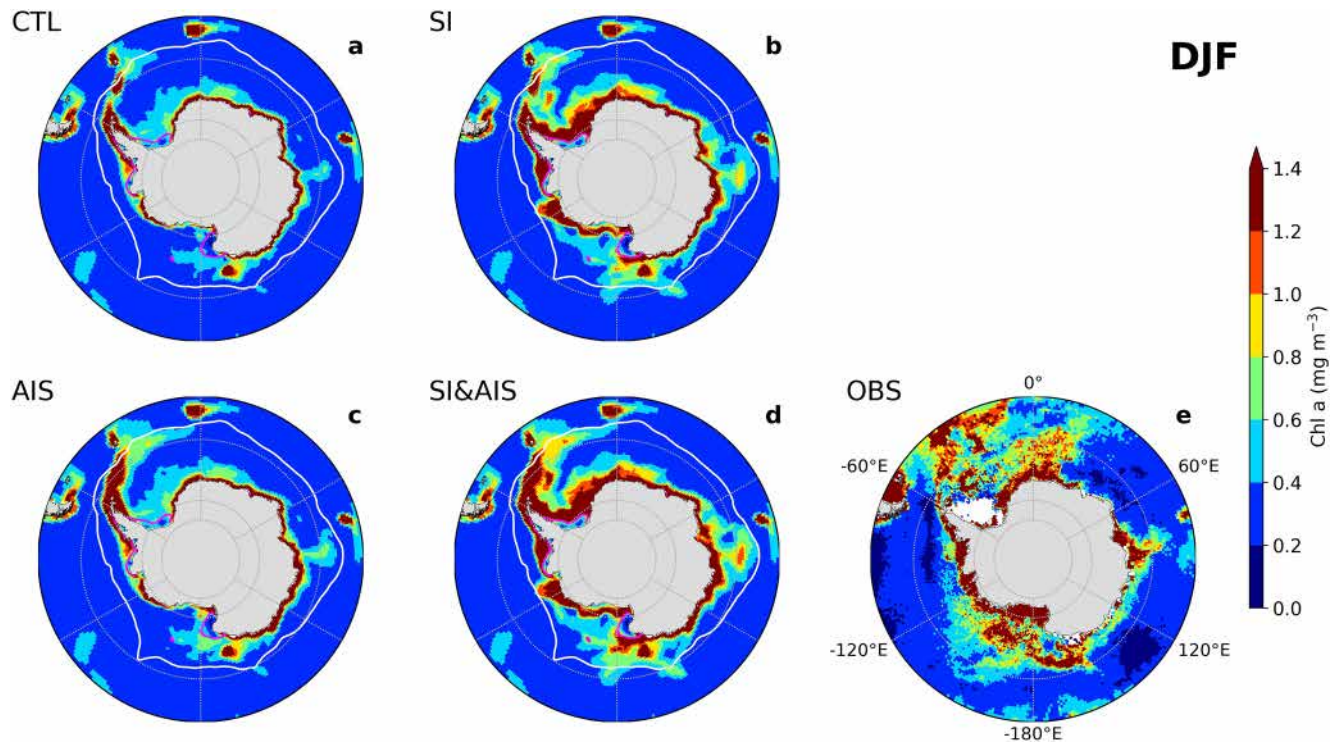


Figure 1. Simulated (a–d) and observed (bottom right) summer (DJF) surface chlorophyll concentrations in the four experiments. Observations are satellite retrievals of surface chlorophyll (2002–2011) from MODIS Aqua (Johnson et al., 2013). Simulated sea-ice edge (15% ice concentration) in September (February) is depicted with a white (magenta) contour. The high iron concentrations along the Antarctic coast in CTL stem from sediment sources.

Hence, each ice Fe source is specific, spatially and temporally, yet both also share many similarities, due to common features in the drift and melt patterns of sea ice and icebergs.

Iron released from sea ice is spread over the Antarctic sea-ice zone (Figure 2a). Sea-ice melt, largely influenced by sea-ice drift, induces a broad, circumpolar coastal to offshore decrease of Fe release, with larger values along the coasts of Antarctica and in the exit limbs of the Weddell and Ross Gyres. The Fe stock in sea ice also plays a role in specific regions, for example, between 25° and 75°E or 110° and 150°E, where simulated Fe concentrations in sea ice and the associated Fe release are generally low. The annual total release of Fe by sea ice is 0.24

Table 1
Key Annual Statistics for the Four Simulations South of 50°S: Depth-Integrated Primary Production (PP), C Export (at 150 m Depth), and Low Production Area (LPA, Defined As the Area Where Primary Production Is Lower Than 25 or 40 mg m⁻² yr⁻¹)

	CTL	SI	AIS	SI&AIS	SI&AIS – (SI + AIS)
PP (TgC yr ⁻¹)	2,327	2,422	2,389	2,498	14.5
Δ (%)		+4.1	+2.6	+7.3	+0.6
C export (TgC yr ⁻¹)	594	642	621	677	8.5
Δ (%)		+8.0	+4.5	+13.9	+1.4
LPA (10 ⁶ km ²)	6.3/16.1	3.8/13.7	5.8/14.9	3.2/12.2	0.2/0.3
Δ (%)		-39/-15	-8/-8	-50/-25	-3/-2
Iron release from cryosphere (Gmol yr ⁻¹)	0	0.24	1.25	1.53	0.04

Note. Changes with respect to CTL (Δ) are expressed in %. The simulated annual Fe release from continental and sea ice sources (sea-ice uptake excluded) is also given. The last column refers to the difference of the simulated anomalies (with respect to CTL) in the SI&AIS experiment and the sum of the corresponding anomalies in the SI and AIS experiments.

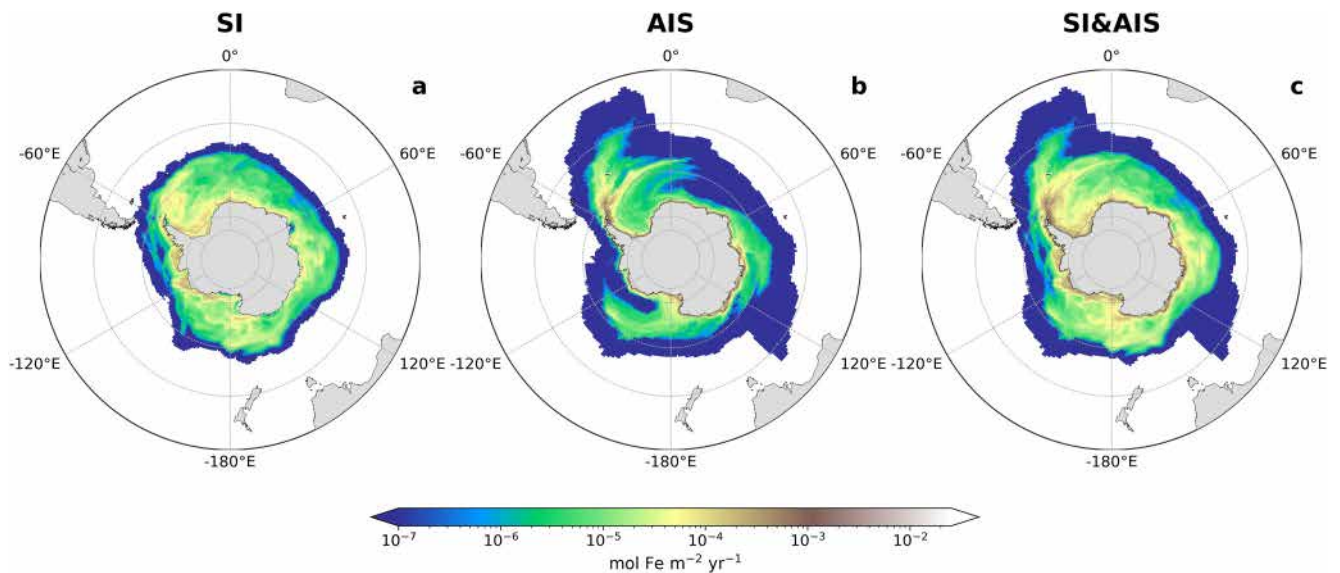


Figure 2. Annual Fe release from continental and sea ice (excluding Fe uptake in sea ice) in the sensitivity experiments: (a) SI, (b) AIS, and (c) SI&AIS.

Gmol yr⁻¹ (Table 1). Iron is released from sea ice during the melt period, that is, between November and February depending on the latitude (Person et al., 2020), and at the surface so that it is readily available to phytoplankton.

Iron released by melting continental ice (Figure 2b) is in comparison more heterogeneous spatially, highly confined around Antarctica and distributed along the trajectories of icebergs in the Atlantic, Ross, and East Antarctic sectors. Continental ice annually releases 1.25 Gmol Fe yr⁻¹, five times more than sea ice, but this Fe is less able to affect primary productivity (Table 1). There are two reasons for this: first, Fe from continental ice is largely released near the coasts where Fe is much less limiting than offshore; second, a significant fraction of this Fe is delivered below the mixed layer, highlighting the influence of injection depth and vertical mixing in the availability of Fe to phytoplankton. Iron released from continental ice peaks between December and February, but is active all year long (Person et al., 2019).

The spatial distribution of Fe released from both forms of ice (Figure 2c) includes the effect of sea-ice melt, which is distributed over the Antarctic sea-ice zone, and the two hotspots where continental and sea ice Fe sources add up: along the Antarctic coasts and east of the tip of the Antarctic Peninsula.

3.3. Continental and Sea Ice Iron Sources Are Coupled

There is a non-linear coupling effect between continental and sea ice: melting ice overall releases 1.53 Gmol Fe yr⁻¹ in SI&AIS, slightly more than the 1.49 Gmol Fe yr⁻¹ obtained from the sum of the individual contributions of continental and sea ice, calculated from AIS and SI (Table 1).

The coupling arises because sea ice is able to store, transport, and release some of the Fe from continental-ice meltwater, a mechanism that prevents this Fe from being lost from the upper ocean, by scavenging for instance. This is further evidenced by Fe concentrations in sea ice being 16% larger with the coupling (in SI&AIS) than without it (in SI). In addition, the differences in Fe concentration within sea ice between SI&AIS and SI mirror continental-ice melt patterns (compare Figures 2c and 3a).

With the coupling (SI&AIS), the simulated mean Fe content in sea ice in November, the month with the largest Fe content in the observations, better matches the observed mean (respectively, 10.6 and 12 μmol m⁻²) than without the coupling (SI, 9.2 μmol m⁻², Table S1 in Supporting Information S1). However, this may not reflect a real model improvement since the Fe content distribution in sea ice, in particular the spread, still largely differs in model and observations (Table S1 in Supporting Information S1).

The continental-sea ice coupling also generally intensifies the impacts of Fe release from both ice forms at the surface. With the coupling, Fe release by melting ice increases the surface ocean Fe concentrations by 18% on

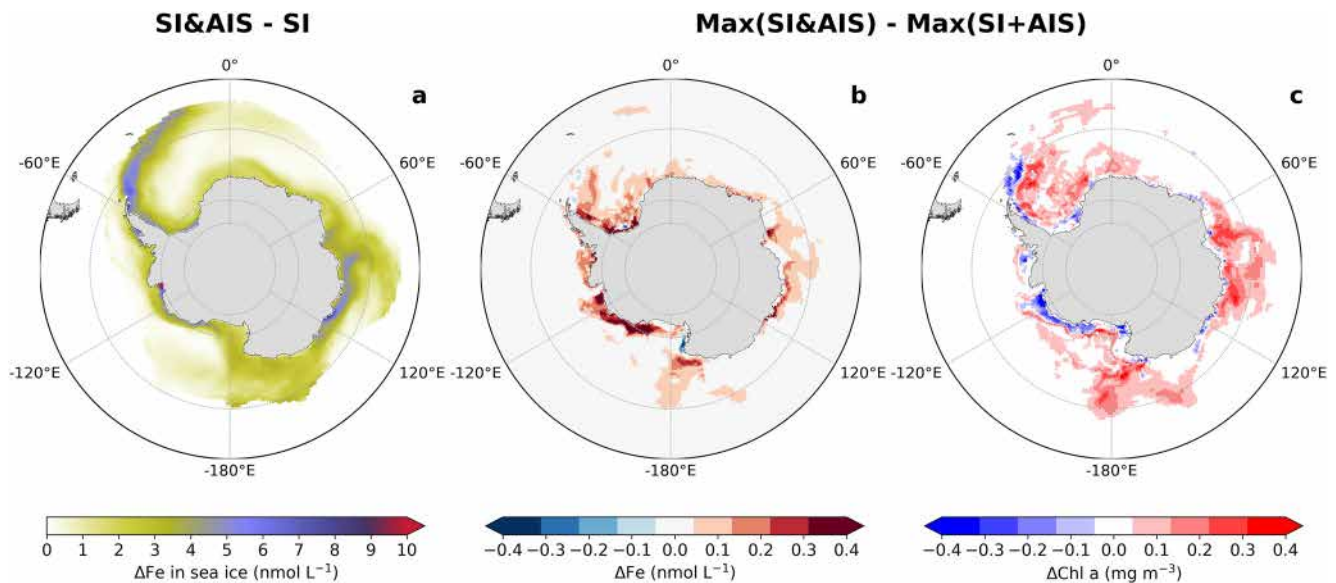


Figure 3. (a) Differences in the annual mean Fe concentration in sea ice between the SI&AIS and SI experiments, highlighting the uptake by sea ice of Fe released by continental ice melting. (b) and (c) Distribution of the coupling effect between continental and sea ice Fe sources; for surface concentrations of (b) Fe and (c) chlorophyll. The coupling effect is defined as the difference of the simulated anomalies (with respect to CTL) in the SI&AIS experiment and the sum of the corresponding anomalies in the SI and AIS experiments. Surface Fe and chlorophyll are taken in the month of their maximum.

average south of 50°S (compare SI&AIS with control). By contrast, the continental and sea ice Fe sources taken separately would sum to 16.5% (we find changes with respect to CTL of 5.5% in SI and 11% in AIS).

Biological activity is also generally higher with the coupling (in SI&AIS) than without. Specifically, the coupling slightly reduces the low production area by $\sim 0.2/0.3$ million km² (Table 1) and increases annual PP and C export by a small fraction of the SO total (1%), which however represents a significant fraction of the total contribution of the two ice-associated Fe sources (+9% for PP, +11.2% for C export).

To further qualify the processes operating the coupling, we compare the fertilization effects with coupling (SI&AIS) to the sum of their individual contributions, without coupling (SI + AIS), when Fe and SChl are maximum (see Figures 3b and 3c and caption for calculation details). The coupling diagnostic indicates a positive effect on surface Fe, in a mean range of 0.1–0.4 nmol L⁻¹ (maximum is 1.2 nmol L⁻¹), mostly around the Antarctic continent, where Fe is not entirely consumed by phytoplankton (Figure 3b). The coupling is also visible in terms of SChl (<0.7 mg m⁻³) in most of the sea-ice zone (Figure 3c) which is generally iron-limited in the control run. The coupling effect is maximum near summer solstice (December and January).

Some regions show negative values of the coupling diagnostic (shown in Figure 3c), indicating that, there, the effect of continental and sea ice Fe sources when coupled is not as large as the sum of their effects when acting separately. The underlying mechanisms depend on the region of interest and generally relate to nutrient limitation. For instance, near the coasts of the Amundsen Sea, the phytoplankton growth is, in our model, not limited by Fe, but by macro-nutrients (Figure S1 in Supporting Information S1). Macro-nutrient stocks cap the extra biomass buildup achievable by Fe fertilization. Maximum biomass is attained in SI&AIS but not in SI or AIS, giving a negative value of the coupling diagnostic. In other regions, for example, near the Atlantic plume and in deep basins off Antarctica, Fe is limiting but not strongly (Figure S2 in Supporting Information S1) and the absence of a coupling is due to subtle non-linearities in the quota formulation of Fe limitation (Aumont et al., 2015).

4. Discussion and Conclusion

How do continental and sea ice Fe sources affect the SO biological carbon pump? When acting together, do their effects combine or saturate? Are there coupling processes between the two sources? The answers found are as follows. (a) Iron from melting ice stimulates phytoplankton activity and increases carbon export by >10% of the SO total. (b) The biological effects of continental and sea ice Fe sources generally combine and overall slightly

reinforce each other when they operate in concert. (c) Such enhancement is attributed to an intensification of the sea-ice Fe source once the continental-ice Fe source is active, which significantly increases Fe in sea ice, and marginally strengthens the biological carbon pump.

As SO phytoplankton is iron-limited during the sea-ice melt season, more active phytoplankton growth upon Fe release by melting ice is consistent with theory and previous works (Lancelot et al., 2009; Laufkötter et al., 2018; Person et al., 2019, 2020). We add here some further credit to that idea. Indeed, Fe released from melting ice stimulates SChl, and remarkably reduces the size of low production areas, by a few million square kilometers. A more intense biological carbon pump associated with more ice favorably echoes satellite and paleotracer studies (Ardyna et al., 2017; Arrigo et al., 2008; Fogwill et al., 2020).

The biological effects resulting from continental and sea ice Fe sources add up because limitation of phytoplankton growth by Fe in the SO is, in our model, strong. Hence, any additional Fe from either source increases phytoplankton growth. The case when the effects of continental and sea ice Fe sources saturate occurs, but rarely, and mostly where macronutrients limit phytoplankton activity.

The coupling effect between continental and sea ice Fe sources arises because some sea ice grows where continental ice melts. Sea ice can therefore incorporate Fe released by melting continental ice, and then transport and release this Fe to locations and times of the year where it more readily increases phytoplankton growth. Such a mechanism is supported by field-based evidence of a contribution from glacial ice melt to Fe in sea ice (Duprat et al., 2020). We find that 16% of Fe in sea ice has a continental-ice origin in our fully coupled simulation, which amounts to $\sim 3\%$ of Fe released by continental-ice melting. This fraction reflects the relative sea-ice volume formed in continental-ice melt-rich waters, and the fraction in these waters of meltwater with continental origin (Merino et al., 2016). The overall impact of this coupling on carbon export is 10% of the contribution of the cryosphere, but 1% of the total SO export.

Our model simulations carry some realism: the emergent mechanisms of Fe transport and supply are compatible with theoretical expectations and the literature and, therefore, deserve some credit. However uncertainties remain large, in particular quantitatively speaking as reality could involve more complex processes (Lannuzel et al., 2016; Raiswell et al., 2018).

Observational constraints on factors key to the biological carbon pump strength are largely lacking. Large uncertainties remain such as Fe concentrations in continental and sea ice, Fe bio-availability to phytoplankton, depth and timing of Fe injection (Hopwood et al., 2019; Lannuzel et al., 2016; Raiswell et al., 2018), satellite estimates of chlorophyll-a in productive coastal regions (e.g., Chen et al., 2021), and limitations by other nutrients (e.g., Mn, see Browning et al., 2021). For instance, iron release from melting ice has significantly different effects with plausible changes in Fe solubility from continental ice (Figure S3 in Supporting Information S1).

Defects in the representation of important model processes can also significantly alter the mechanisms we present. The simulated chlorophyll distribution has clear deficiencies and the summer sea-ice cover is underestimated (Figure 1). The effects of important processes have not been carefully evaluated or tuned, in particular vertical mixing under sea ice, which controls Fe supply, possibly Fe uptake into sea ice, and light limitation upon Fe release. Others possibly important model processes are missing such as Fe-rich sea-ice types (Fraser et al., 2012; Hoppmann et al., 2020) or ice algae. Resolution is also insufficient to capture the details of the model response, in particular near icebergs and ice shelf mouths.

Nevertheless, this study confirms and precises the role of the Antarctic cryosphere as a major environmental driver of phytoplankton activity in the SO. Continental and sea ice Fe sources are different but can be seen as acting in synergy, as their effects superpose and complement each other. Ice transport processes emerge as central, hence they could be key to understand variability and recent changes in phytoplankton activity in the SO (Montes-Hugo et al., 2009; Moreau et al., 2015; Pinkerton et al., 2021). Large areas of progress are envisioned in observational and modeling research activities, both in terms of physics and biogeochemistry of the Antarctic marine environment.

Data Availability Statement

Model data are available at Zenodo (<http://doi.org/10.5281/zenodo.4904837>). Sea-ice Fe data are available online (<https://doi.pangaea.de/10.1594/PANGAEA.865037>). The authors thank R. Raiswell and three anonymous reviewers for their comments and Sébastien Moreau for discussion.

Acknowledgments

This work is funded by the SOBUMS ANR project (ANR-16-CE01-0014) and was granted access to IDRIS HPC resources under the GENCI 2020-A0080107451 allocation.

References

- Ardyna, M., Claustre, H., Sallée, J.-B., D'Ovidio, F., Gentili, B., van Dijken, G., et al. (2017). Delineating environmental control of phytoplankton biomass and phenology in the Southern Ocean. *Geophysical Research Letters*, *44*, 5016–5024. <https://doi.org/10.1002/2016GL072428>
- Arrigo, K. R., van Dijken, G. L., & Bushinsky, S. (2008). Primary production in the Southern Ocean, 1997–2006. *Journal of Geophysical Research*, *113*(C8). <https://doi.org/10.1029/2007JC004551>
- Arrigo, K. R., van Dijken, G. L., & Strong, A. L. (2015). Environmental controls of marine productivity hot spots around Antarctica. *Journal of Geophysical Research: Oceans*, *120*(8), 5545–5565. <https://doi.org/10.1002/2015JC010888>
- Arrigo, K. R., Worthen, D. L., Lizotte, M. P., Dixon, P., & Dieckmann, G. (1997). Primary production in Antarctic Sea ice. *Science*, *276*(5311), 394–397. <https://doi.org/10.1126/science.276.5311.394>
- Aumont, O., Ethé, C., Tagliabue, A., Bopp, L., & Gehlen, M. (2015). PISCES-v2: An ocean biogeochemical model for carbon and ecosystem studies. *Geoscientific Model Development*, *8*(8), 2465–2513. <https://doi.org/10.5194/gmd-8-2465-2015>
- Bintanja, R., van Oldenborgh, G. J., Drijfhout, S. S., Wouters, B., & Katsman, C. A. (2013). Important role for ocean warming and increased ice-shelf melt in Antarctic sea-ice expansion. *Nature Geoscience*, *6*(5), 376–379. <https://doi.org/10.1038/NNGEO1767>
- Boyd, P. W., & Ellwood, M. J. (2010). The biogeochemical cycle of iron in the ocean. *Nature Geoscience*, *3*(10), 675–682. <https://doi.org/10.1038/ngeo964>
- Boyd, P. W., Jickells, T., Law, C. S., Blain, S., Boyle, E. A., Buesseler, K. O., et al. (2007). Mesoscale iron enrichment experiments 1993–2005: Synthesis and future directions. *Science*, *315*(5812), 612–617. <https://doi.org/10.1126/science.1131669>
- Browning, T. J., Achterberg, E. P., Engel, A., & Mawji, E. (2021). Manganese co-limitation of phytoplankton growth and major nutrient draw-down in the Southern Ocean. *Nature Communications*, *12*(1), 1–9. <https://doi.org/10.1038/s41467-021-21122-6>
- Chen, S., Smith, W. O., Jr., & Yu, X. (2021). Revisiting the ocean color algorithms for particulate organic carbon and chlorophyll-a concentrations in the Ross Sea. *Journal of Geophysical Research: Oceans*, *126*(8), e2021JC017749. <https://doi.org/10.1029/2021JC017749>
- de Jong, J., Schoemann, V., Maricq, N., Mattielli, N., Langhorne, P., Haskell, T., & Tison, J.-L. (2013). Iron in land-fast sea ice of McMurdo Sound derived from sediment resuspension and wind-blown dust attributes to primary productivity in the Ross Sea, Antarctica. *Marine Chemistry*, *157*, 24–40. <https://doi.org/10.1016/j.marchem.2013.07.001>
- Death, R., Wadham, J. L., Monteiro, F., Le Brocq, A. M., Tranter, M., Ridgwell, A., et al. (2014). Antarctic ice sheet fertilises the Southern Ocean. *Biogeosciences*, *11*(10), 2635–2643. <https://doi.org/10.5194/bg-11-2635-2014>
- Depoorter, M. A., Bamber, J. L., Griggs, J. A., Lenaerts, J. T. M., Ligtenberg, S. R. M., van den Broeke, M. R., & Moholdt, G. (2013). Calving fluxes and basal melt rates of Antarctic ice shelves. *Nature*, *502*(7469), 89–92. <https://doi.org/10.1038/nature12567>
- Dinniman, M. S., St-Laurent, P., Arrigo, K. R., Hofmann, E. E., & Dijken, G. L. V. (2020). Analysis of iron sources in Antarctic continental shelf waters. *Journal of Geophysical Research: Oceans*, *125*(5), e2019JC015736. <https://doi.org/10.1029/2019JC015736>
- Duprat, L., Corkill, M., Genovese, C., Townsend, A. T., Moreau, S., Meiners, K. M., & Lannuzel, D. (2020). Nutrient distribution in east Antarctic summer sea ice: A potential iron contribution from glacial basal melt. *Journal of Geophysical Research: Oceans*, *125*(12). <https://doi.org/10.1029/2020JC016130>
- Fogwill, C. J., Turney, C. S. M., Menviel, L., Baker, A., Weber, M. E., Ellis, B., et al. (2020). Southern Ocean carbon sink enhanced by sea-ice feedbacks at the Antarctic cold reversal. *Nature Geoscience*, *13*(7), 489–497. <https://doi.org/10.1038/s41561-020-0587-0>
- Fraser, A. D., Massom, R. A., Michael, K. J., Galton-Fenzi, B. K., & Lieser, J. L. (2012). East Antarctic landfast sea ice distribution and variability, 2000–08. *Journal of Climate*, *25*(4), 1137–1156. <https://doi.org/10.1175/JCLI-D-10-05032.1>
- García, H. E., Locarnini, R. A., Boyer, T. P., Antonov, J. I., Zweng, M. M., Baranova, O. K., & Johnson, D. R. (2010a). World Ocean Atlas 2009 volume 3: Dissolved oxygen, apparent oxygen utilization, and oxygen saturation. In *NOAA Atlas NESDIS* (Vol. 70). U.S. Government Printing Office.
- García, H. E., Locarnini, R. A., Boyer, T. P., Antonov, J. I., Zweng, M. M., Baranova, O. K., & Johnson, D. R. (2010b). World Ocean Atlas 2009 volume 4: Nutrients (phosphate, nitrate, silicate). In *NOAA Atlas NESDIS* (Vol. 71). U.S. Government Printing Office.
- Griffies, S. M., Biastoch, A., Böning, C., Bryan, F., Danabasoglu, G., Chassignet, E. P., et al. (2009). Coordinated ocean-ice reference experiments (COREs). *Ocean Modelling*, *26*(1–2), 1–46. <https://doi.org/10.1016/j.ocemod.2008.08.007>
- Hoppmann, M., Richter, M. E., Smith, I. J., Jendersie, S., Langhorne, P. J., Thomas, D. N., & Dieckmann, G. S. (2020). Platelet ice, the Southern Ocean's hidden ice: A review. *Annals of Glaciology*, *61*, 1–368. <https://doi.org/10.1017/aog.2020.54>
- Hopwood, M. J., Carroll, D., Höfer, J., Achterberg, E. P., Meire, L., Le Moigne, F. A. C., et al. (2019). Highly variable iron content modulates ice-berg-ocean fertilisation and potential carbon export. *Nature Communications*, *10*(1), 5261. <https://doi.org/10.1038/s41467-019-13231-0>
- Johnson, R., Strutton, P. G., Wright, S. W., McMinn, A., & Meiners, K. M. (2013). Three improved satellite chlorophyll algorithms for the Southern Ocean. *Journal of Geophysical Research: Oceans*, *118*(7), 3694–3703. <https://doi.org/10.1002/jgrc.20270>
- Key, R. M., Kozyr, A., Sabine, C. L., Lee, K., Wanninkhof, R., Bullister, J. L., & Peng, T.-H. (2004). A global ocean carbon climatology: Results from global data analysis project (GLODAP). *Global Biogeochemical Cycles*, *18*(4). <https://doi.org/10.1029/2004gb002247>
- Lancelot, C., Montety, A. D., Goosse, H., Becquevort, S., Schoemann, V., Pasquer, B., & Vancoppenolle, M. (2009). Spatial distribution of the iron supply to phytoplankton in the Southern Ocean: A model study. *Biogeosciences*, *6*(12), 2861–2878. <https://doi.org/10.5194/bg-6-2861-2009>
- Lannuzel, D., Vancoppenolle, M., van der Merwe, P., de Jong, J., Meiners, K., Grotti, M., et al. (2016). Iron in sea ice: Review and new insights. *Elementa: Science of the Anthropocene*, *4*, 000130. <https://doi.org/10.12952/journal.elementa.000130>
- Laufkötter, C., Stern, A. A., John, J. G., Stock, C. A., & Dunne, J. P. (2018). Glacial iron sources stimulate the Southern Ocean carbon cycle. *Geophysical Research Letters*, *45*(24377–13), 13385. <https://doi.org/10.1029/2018GL079797>
- Lin, H., Rauschenberg, S., Hexel, C. R., Shaw, T. J., & Twining, B. S. (2011). Free-drifting icebergs as sources of iron to the Weddell Sea. *Deep Sea Research Part II: Topical Studies in Oceanography*, *58*(11–12), 1392–1406. <https://doi.org/10.1016/j.dsr2.2010.11.020>
- Locarnini, R. A., Mishonov, A. V., Antonov, J. I., Boyer, T. P., García, H. E., Baranova, O. K., & Seidov, D. (2013). World Ocean Atlas 2013, Volume 1: Temperature. *NOAA Atlas NESDIS*, *73*, 40.
- Madec, G. (2008). *NEMO ocean engine* (Vol. 27, pp. 1–217). Note du pole de modélisation de l'Institut Pierre-Simon Laplace.

- Martin, J. H. (1990). Glacial-interglacial CO₂ change: The iron hypothesis. *Paleoceanography*, 5(1), 1–13. <https://doi.org/10.1029/pa005i001p00001>
- Mathiot, P., Jenkins, A., Harris, C., & Madec, G. (2017). Explicit representation and parametrised impacts of under ice shelf seas in the z coordinate ocean model NEMO 3.6. *Geoscientific Model Development*, 10(7), 2849–2874. <https://doi.org/10.5194/gmd-10-2849-2017>
- Merino, N., Le Sommer, J., Durand, G., Jourdain, N. C., Madec, G., Mathiot, P., & Tournadre, J. (2016). Antarctic icebergs melt over the Southern Ocean: Climatology and impact on sea ice. *Ocean Modelling*, 104, 99–110. <https://doi.org/10.1016/j.ocemod.2016.05.001>
- Montes-Hugo, M., Doney, S. C., Ducklow, H. W., Fraser, W., Martinson, D., Stammerjohn, S. E., & Schofield, O. (2009). Recent changes in phytoplankton communities associated with rapid regional climate change along the western Antarctic peninsula. *Science*, 323(5920), 1470–1473. <https://doi.org/10.1126/science.1164533>
- Moreau, S., Mostajir, B., Bélanger, S., Schloss, I. R., Vancoppenolle, M., Demers, S., & Ferreyra, G. A. (2015). Climate change enhances primary production in the western Antarctic Peninsula. *Global Change Biology*, 21(6), 2191–2205. <https://doi.org/10.1111/gcb.12878>
- Noble, A. E., Moran, D. M., Allen, A. E., & Saito, M. A. (2013). Dissolved and particulate trace metal micronutrients under the McMurdo Sound seasonal sea ice: Basal sea ice communities as a capacitor for iron. *Frontiers in Chemistry*, 1. <https://doi.org/10.3389/fchem.2013.00025>
- Person, R., Aumont, O., Madec, G., Vancoppenolle, M., Bopp, L., & Merino, N. (2019). Sensitivity of ocean biogeochemistry to the iron supply from the Antarctic Ice Sheet explored with a biogeochemical model. *Biogeosciences*, 16(18), 3583–3603. <https://doi.org/10.5194/bg-16-3583-2019>
- Person, R., Vancoppenolle, M., & Aumont, O. (2020). Iron incorporation from seawater into Antarctic Sea ice: A model study. *Global Biogeochemical Cycles*, 34(11). <https://doi.org/10.1029/2020GB006665>
- Pinkerton, M. H., Boyd, P. W., Deppeler, S., Hayward, A., Höfer, J., & Moreau, S. (2021). Evidence for the impact of climate change on primary producers in the Southern Ocean. *Frontiers in Ecology and Evolution*, 9, 592027. <https://doi.org/10.3389/fevo.2021.592027>
- Raiswell, R., Hawkings, J., Elsenously, A., Death, R., Tranter, M., & Wadham, J. (2018). Iron in glacial systems: Speciation, reactivity, freezing behavior, and alteration during transport. *Frontiers of Earth Science*, 6(222). <https://doi.org/10.3389/feart.2018.00222>
- Raiswell, R., Hawkings, J. R., Benning, L. G., Baker, A. R., Death, R., Albani, S., et al. (2016). Potentially bioavailable iron delivery by ice-berg-hosted sediments and atmospheric dust to the polar oceans. *Biogeosciences*, 13(13), 3887–3900. <https://doi.org/10.5194/bg-13-3887-2016>
- Rousset, C., Vancoppenolle, M., Madec, G., Fichefet, T., Flavoni, S., Barthélemy, A., et al. (2015). The Louvain-La-Neuve sea ice model LIM3.6: Global and regional capabilities. *Geoscientific Model Development*, 16, 2991–3005. <https://doi.org/10.5194/gmd-8-2991-2015>
- Sedwick, P. N., & DiTullio, G. R. (1997). Regulation of algal blooms in Antarctic Shelf Waters by the release of iron from melting sea ice. *Geophysical Research Letters*, 24(20), 2515–2518. <https://doi.org/10.1029/97GL02596>
- St-Laurent, P., Yager, P. L., Sherrell, R. M., Stammerjohn, S. E., & Dinniman, M. S. (2017). Pathways and supply of dissolved iron in the Amundsen Sea (Antarctica). *Journal of Geophysical Research: Oceans*, 122(9), 7135–7162. <https://doi.org/10.1002/2017JC013162>
- Tamura, T., Ohshima, K. I., Fraser, A. D., & Williams, G. D. (2016). Sea ice production variability in Antarctic coastal polynyas. *Journal of Geophysical Research: Oceans*, 121(5), 2967–2979. <https://doi.org/10.1002/2015JC011537>
- Vancoppenolle, M., Fichefet, T., Goosse, H., Bouillon, S., Madec, G., & Maqueda, M. A. M. (2009). Simulating the mass balance and salinity of Arctic and Antarctic sea ice. 1. Model description and validation. *Ocean Modelling*, 27(1–2), 33–53. <https://doi.org/10.1016/j.ocemod.2008.10.005>
- Wadley, M. R., Jickells, T. D., & Heywood, K. J. (2014). The role of iron sources and transport for Southern Ocean productivity. *Deep Sea Research Part I: Oceanographic Research Papers*, 87, 82–94. <https://doi.org/10.1016/j.dsr.2014.02.003>
- Wang, S., Bailey, D., Lindsay, K., Moore, J. K., & Holland, M. (2014). Impact of sea ice on the marine iron cycle and phytoplankton productivity. *Biogeosciences*, 11(17), 4713–4731. <https://doi.org/10.5194/bg-11-4713-2014>
- Zweng, M. M., Reagan, J. R., Antonov, J. I., Locarnini, R. A., Mishonov, A. V., Boyer, T. P., & Biddle, M. M. (2013). World Ocean Atlas 2013, volume 2: Salinity. *NOAA Atlas NESDIS*, 74, 39.